Optica Applicata, Vol. XLIX, No. 1, 2019
DOI: 10.5277/oa190108

Adaptive lighting for inhomogeneous reflectivity compensation in applications for 3D shape measurements

Caterina CASAVOLA, Giovanni PAPPALETTERA*

Politecnico di Bari, Dipartimento di Meccanica, Matematica, Management,
Viale Japigia 182, 70126 Bari, Italy

*Corresponding author: giovanni.pappalettera@poliba.it

Surface 3D reconstruction is a topic of great relevance and it has a wide range of applications in many fields such as mechanics, bioengineering and arts. Nowadays optical systems for 3D contouring such as those based on structured light projection are becoming more and more widespread. The possibility to get shape information without any contact with the object, in fact, is a great advantage in some fields such as, for example, cultural heritage. For this class of objects, however, the issue connected with inhomogeneous reflectivity must be taken into account. Due to the different level of reflectivity, in different areas of the object, it comes out that the contrast of the projected pattern changes and, as a direct consequence, the achievable accuracy can change from part to part. In this paper, a study on the possibility to implement an adaptive lighting algorithm is performed allowing to adapt illumination in order to compensate the local inhomogeneities in terms of surface reflectivity.

Keywords: fringe projection, structured light projection, surface reflectivity, 3D contouring.

1. Introduction

In recent years, the production of digital models of real objects is becoming very important in different areas such as mechanical design, dimensional control, quality control, industrial design, bioengineering and the cultural heritage preservation.

Reverse engineering allows obtaining, as a final output, a file representing a digital copy of the object that can be edited by modern CAD/CAM software. The shape acquisition systems can be divided into two main categories [1]: those based on contact techniques and those based on non-contact techniques. The former have an accuracy that can reach typically about 0.5 μm to be compared with 10 μm of accuracy usually achievable by optical technologies [2]. This difference mainly depends on the fact that, in the first case, the detection is performed touching the surface point by point with a probe whose motion is electronically controlled with a very high level of accuracy. The entire process and instrumentation needed is very complex and is characterized by low data acquisition speed and high costs. It should also be taken into account that there are some situations where contact probe techniques are not applicable. This can happen, for example, when dealing with soft material or with cultural heritage objects. In this case, the non-contact techniques, based on optical technology, are preferable.

The optical techniques can be divided into two types, depending on the mode of interaction with the physical shape of the object and the type of light source used. The first strategy, known as passive optical acquisition, tries to analyze the 3D scene under ambient light. The most widespread is the photogrammetry that allows obtaining high levels of accuracy but it requires long times for the data processing, a delicate operation of system calibration and application of markers [3]. The second one, known as active optical acquisition, includes light pattern projection over the surface of the object to be analyzed, while a CCD camera is adopted to detect light reflected by the object [4, 5]. The shape of the object introduces a modulation of the projected pattern; if the information recorded is properly demodulated, then it is possible to extract the shape of the examined object, creating a unique match between the image pixels and the points analyzed in the physical space. The determination of the coordinates of the surface of an object is obtained through the triangulation method [6–9]. In principle, whatever pattern can be projected, however usually a sinusoidal pattern of vertical or horizontal lines is adopted. The accuracy of the technique is a function of the features of the projected pattern [10]. The quality of the measurement can be improved by using the temporal phase shifting (TPS) technique, which involves the projection of fringes which are shifted by given phase value. Accuracy of the measurement can be further increased by introducing proper calibration procedures to take into account lens aberrations [11]; in such a way, a level of accuracy of 1/1000 of the measurement volume can be obtained.

However, it must be taken into account that surface reflectivity conditions of the analyzed object can drastically deteriorate the quality of the measurements. In order to obtain high accuracy, the contrast of the projected pattern must be good and it should be optimized by a proper setting of the illumination intensity and of the camera acquisition parameters such as gain and shutter time. In particular, highly reflective surfaces are difficult to capture because they produce a series of artifacts that lead to the generation of particularly noisy clouds due to saturation. On the opposite side, opaque surfaces cause a reduction in contrast. This compromises the regularity of the pattern [12]. Global optimization, which can be also obtained by optimizing overall projected intensity as it, is reported in [13, 14]. However this approach fails when regions of different reflectivity are present and a tradeoff must be reached in order to get enough illumination in the dark areas avoiding, at the same time, saturation effects in the most reflective regions. A possible solution involves the application of a thin layer of whitening product to make the whole surface homogeneous. However, for some applications (*e.g.*, cultural heritage or bioengineering) the introduction of a spray is not possible. In literature, several works have been developed to solve the problem of surface reflectivity [15]. For example, a type of modified clustering algorithm was created to evaluate the region of interest and to remove specular reflection [16] or, as the image of an object can vary dramatically depending on lighting, specular reflections and shadows, it is often advantageous to separate these incidental variations from the intrinsic aspects of an image [17]. Furthermore, a new dual sensing measuring method for 3D surface profilometry was developed to deal with the problem of performing measurement on an object with inhomogeneous reflectivity. This technique is based on a new optical configuration to simultaneously detect specular and diffuse light reflected from various surface regions on the tested object [18]. Optimization at a pixel level was presented in [19]. In this work, phase shifting of a given projected pattern was implemented and pixel by pixel intensity-modulation for a given initial maximum gray level was studied. If a pixel can be classified as unsaturated, the information is saved at that stage. Successively illumination is globally reduced and again intensity-modulation is checked and information of new unsaturated pixel is saved. At the end of the process, a composite image is composed made up of the information recorded at each step. Also in [20] an analogous approach of illumination optimization at a pixel level is proposed where correspondence between camera and projector pixel is determined by a calibration procedure using a checkerboard. HUI LIN *et al.* [21] developed a procedure to adapt illumination at a pixel level, however in their algorithm a complex approach requiring phase calculation for unsatured pixel is proposed; moreover for a dark region, the optimization is performed just by setting at the maximum the illumination level. Finally the concept of adaptive illumination at a pixel level was also followed by CHI ZHANG *et al.* [22]. In particular their approach is based on an initial guess of the spread function based on the assumption that the object is a flat plane. Variation of intensity is performed at a pixel level to adapt illumination to the surface condition, if the number of bad pixels overcome a given threshold (that can be obtained if flatness of the object is very low), point spread function is adjusted iteratively.

In this paper, an approach to homogenize the quantity of reflected radiation is proposed based upon the implementation of an adaptive lighting algorithm that varies locally the lighting level to compensate differences in terms of reflectivity of the object under examination. The approach is based upon the definition of a given range of acceptance in terms of recorded intensity. If the intensity, at a given pixel, falls within that interval no change occurs, otherwise illumination for that specific pixel is changed adaptively. Image recorded by the camera is used to perform the control and illumination is changed locally to compensate inhomogeneity. Differently from [19] intensity is varied at pixel level while differently from [20] and [22] the process to determine camera/projector pixel correspondence is simplified and it does not make use of a checkerboard or iterative calculations.

2. 2. Material and methods

A typical set-up for fringe projection in a classical triangulation scheme was built as displayed in Fig. 1. The set-up of measure consists of a standard CCD camera with a resolution of 2452 × 2056 pixels, a frame rate of 9 fps, an ADC of 8 bit and an LCD pro-

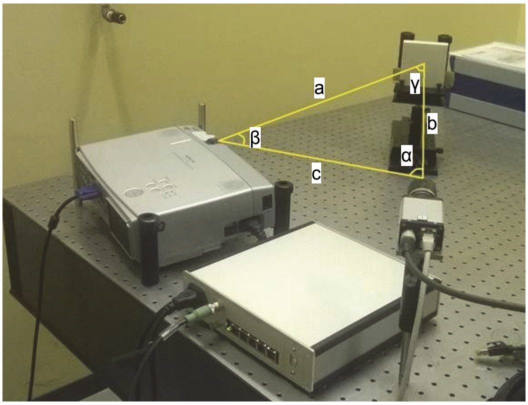

Fig. 1. Picture of the fringe projection set-up in triangulation scheme.

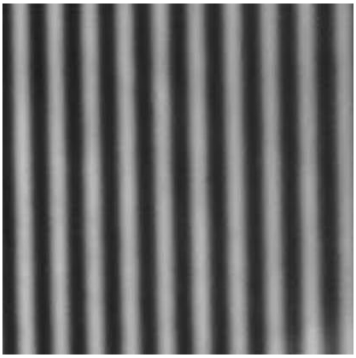

Fig. 2. Fringe pattern projected on the reference plane and recorded by the CCD camera.

jector with a resolution of 1024 × 768 pixels. The camera was equipped with an optics with a focal ratio of 2.8 and a focal length of 50.2 mm. These are quite common and typical components for these kind of systems.

The fixed geometric parameters are the distance between the camera and the projector, equal to 530 mm, and the angle between camera and projector which was set to 45°. Also in this case, these are quite commons geometrical settings for triangulation system.

A pattern with a frequency equal to 0.1 fringe/pixel was projected over a flat reference surface and focus adjustments of camera and projector as well as shutter time and gain of the camera were set in order to obtain good contrast on the reference plane (Fig. 2).

As it can be inferred, due to the homogeneous conditions of the reference surface, the contrast is high in every part of the surface.

The algorithm to detect the presence of areas with different degrees of illumination and the local variation of the level of illumination was implemented in LabView according with the workflow reported in Fig. 3.

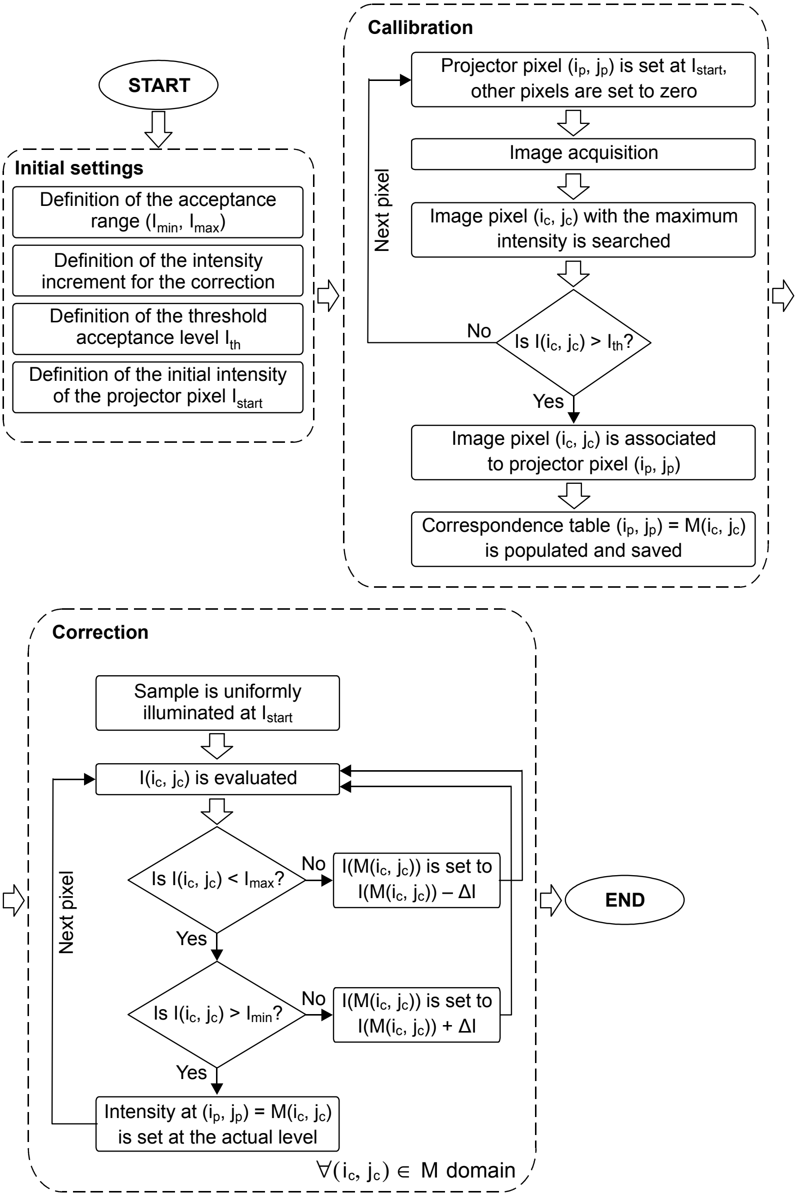

Fig. 3. Flowchart of the adaptive lighting algorithm: initial settings, calibration and correction steps.

This algorithm allows detecting the inhomogeneities of areas in terms of reflectivity, and allows a correction based on local lighting variation. The algorithm consists of three steps. In the first step, the algorithm takes into account the affine transformations among projector and camera pixels in the following way: single projection pixels $(i_\mathrm{p}, j_\mathrm{p})$ are illuminated in sequence; this will correspond to illumination of the corresponding (i_c, j_c) in the camera image reference system. In this way it is possible to generate a lookup table that allows connecting any pixel of the projector to any pixel of the camera. It should be underlined that due to different resolution between projection and camera systems a mismatch occurs. Moreover, the extension of the field of illumination is larger than the extension of the field of view. To overcome this issue at each (i_p, j_p) projected pixel, the (i_c, j_c) where the maximum intensity is recorded is associated. A threshold is set to avoid false association in correspondence of projected pixels that falls out from the camera field of view. If the intensity does not overcome that threshold level in any pixel of the recorded image no association occurs, and the projected pixel is considered out from the region of interest. The second step is the monitoring. In this step, the object is illuminated by starting with an homogeneous level of illumination. If the object has an inhomogeneous reflectivity, the intensity of the recorded image can vary from pixel to pixel. The recorded level of intensity for each pixel is compared with a maximum and minimum level of reference which is defined by the user and given as an input to the software. If the intensity value for a given (i_c, j_c) pixel is out from the user defined range than a correction is performed (step 3) that is to say that a $\pm\Delta I$ is added to the corresponding (i_p, j_p) pixel. The amount of $\pm\Delta I$ is defined by the user and it is given as an input to the algorithm. Step 2 and step 3 are performed iteratively until a level of intensity within the user defined limits is recorded for all the pixels of the image.

In order to validate the proposed approach, measurements were performed on a sample object. This consisted of a cylindrical surface having an homogeneous level of reflectivity. Two measurements were performed on the object. Firstly 3D shape measurement was performed following the approach based on fringe phase shifting as described in [23] and the phase calibration procedure reported in [24]. Initial measurement was performed on the object as it is; then surface of the object was modified in two areas so that a darker area and a brighter area was painted on it and the measurement was repeated (Fig. 4).

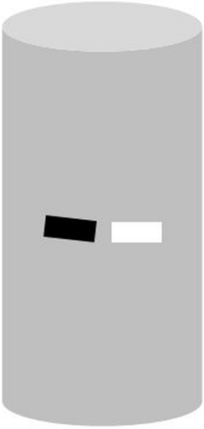

Fig. 4. Scheme of the object employed for the 3D measurement test with and without algorithm.

Two measurements were performed. In the first one, the same sinusoidal patterns as in the previous measurements are projected. In the second one, the sinusoidal pattern is modulated by the $I(i_c, j_c)$ function as obtained by the implemented algorithm. Comparison among obtained results is shown in the next section.

3. Results and discussion

In order to check the possibility to use the proposed algorithm to homogenize the level of recorded intensity, a test was performed on a sample where regions of different reflectivity were artificially created.

Camera settings were adjusted so that background intensity is about 127 (grayscale level) that is to say in the middle of the dynamic range allowed by the camera.

Region of higher reflectivity and lower reflectivity were created *ad hoc* on the surface in the shape of regular geometric figures by painting different areas of the sample by white and dark gray paints. In the upper left part of the Fig. 5 it is possible to observe the initial state that is to say the first image captured by the CCD camera. As an effect of the uniform illumination and the presence of regions of different reflectivity, the image displays regions with different level of intensities.

If the algorithm is made to run iteratively, it is possible to arrive to a more homogeneous situation how it is observable in the upper right part of Fig. 5. In particular, for the given settings $\Delta I = \pm 10$, twelve iterations were required to reach the situation described in the right part of Fig. 5. In the lower part of Fig. 5, it is possible to quantify the action of the algorithm. As an example, a horizontal cross-section is examined as

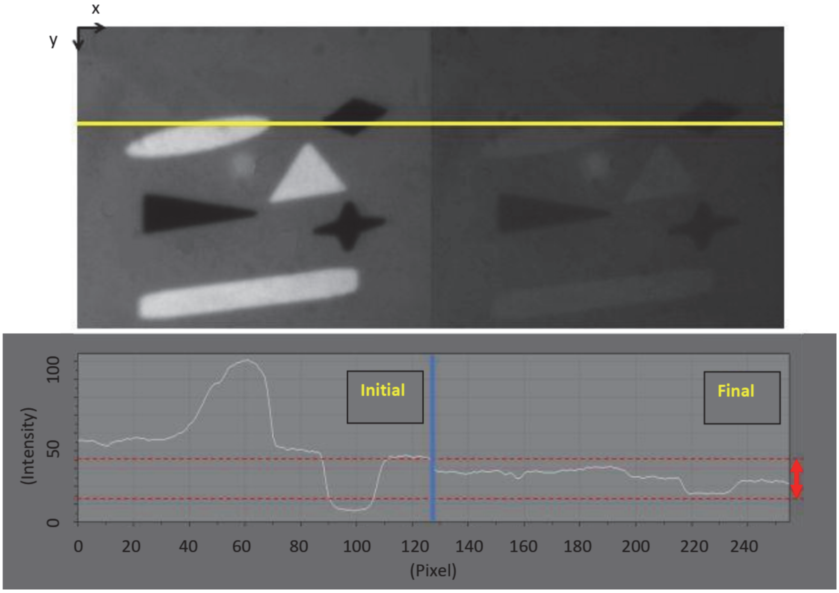

Fig. 5. Simulation of process of adaptive lighting algorithm.

indicated by the yellow line. In the lower part of Fig. 5, it is possible to observe intensity variation before starting the local adaptation process of the illumination and at the end of the process. The dashed lines indicates the specific acceptance range adopted for this test. Based on same preliminary evaluation we decided that an acceptance level of 50 gray levels that is to say 5 times the $\pm\Delta I$ used in this experiment was a good compromise to get sufficient homogeneity in a reasonable amount of time. It is worth noting that even if the acceptance range was set far from the initial intensity levels in the brightest areas, the algorithm acted efficiently also in that regions. Once that the compensation algorithm has been run, it is possible to obtain the compensation matrix $A_c(i,j)$. These matrix coefficients can be multiplied by the projection pattern in order to obtain a compensated projected pattern (Fig. 6).

It is possible to observe that the contrast of the projected pattern is much more uniform if compensation is actuated.

Compensation of the illumination allows to find better adjustments of the gain and shutter time parameters that allow exploiting better the CCD dynamic range. By observing the cross-sections of the projected patterns (Fig. 7) before and after the compensation, it is possible to observe that initially, in correspondence of the darker areas,

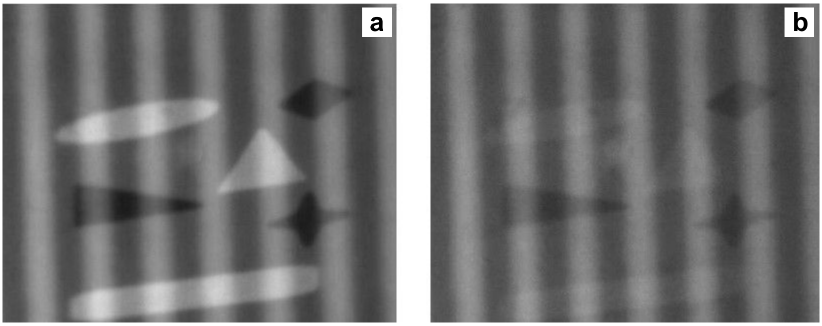

Fig. 6. Projected pattern: without (**a**) and with (**b**) compensation algorithm.

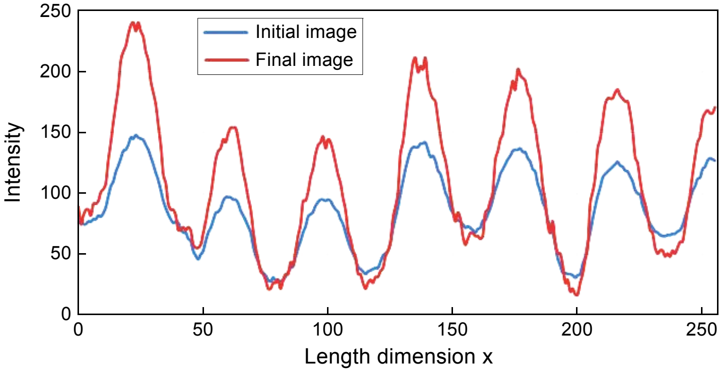

Fig. 7. Comparison of the intensity patterns before and after the correction.

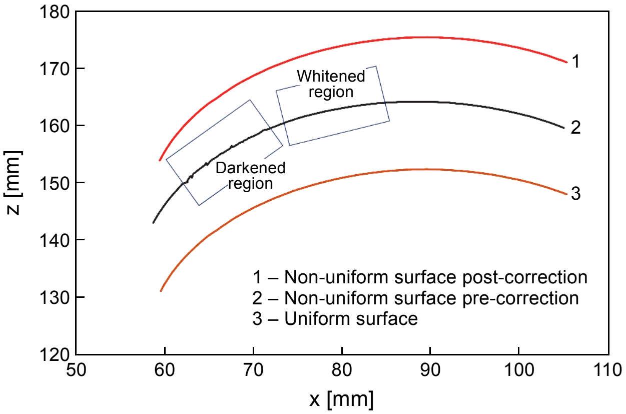

Fig. 8. Comparative 3D measurement on cylindrical surface. Measurement was performed initially on the uniform surface. Later two areas were painted with lower and higher reflectivity and measurements were repeated with and without the implemented algorithm.

the signal spans over about 75 gray levels, while, after compensation, in the low contrast areas, the signal covers almost 125 gray levels.

At the same time no saturation occurs in the more reflective regions. It is worth reminding that the actual achievable sensitivity with fringe projection methods is given by the sensitivity per fringe S_f divided by the number of gray levels covered by the signal. This directly means that the proposed approach allows reducing sensitivity, that is to say to reduce the minimum detectable out-of-plane displacement more than 60% with respect to the original situation.

Preliminary indications about capability of the proposed algorithm can be inferred by Fig.8 where results of the measurement on a cylindrical surface are reported as obtained along a cross-section crossing the two areas of different reflectivity. The three curves were shifted to facilitate visualization. It is possible to observe that when areas of different reflectivity are introduced variations from the initial profile appear. In particular, for the analyzed case they are evident in the region of lower reflectivity while they are absent in the case of higher reflectivity. This can be explained by considering that the contrast is sufficient enough to guarantee accurate measurement but, at the same time, reflectivity is not so high to introduce issues connected with saturation. However if algorithm is implemented and intensity is conveniently adapted then again, how it can be observed by looking at the curve 1 in Fig. 8, the correct shape can be recovered everywhere overcoming problems connected with low contrast.

4. Conclusions and future works

Presence of regions of different reflectivity can be a problem when dealing with optical methods. In particular, when operating with fringe projections methods, the contrast of the projected pattern can heavily reduce. Global optimization of the CCD camera acquisition parameters must be performed and it must balance the necessity to avoid saturation in the most reflective areas and to guarantee enough illumination in the low reflective areas. However with this approach, the contrast cannot be locally optimized.

In this paper, a preliminary study about the possibility to obtain adaptive compensation of the illumination is proposed. Image of the surface is acquired and this is used as a control in order to compensate pixel by pixel the level of illumination. Projected intensity is increased in the dark region and decreased in the brighter region until recorded intensity levels fall within a user defined acceptance range. It has been demonstrated that this approach in homogenizing the contrast of the projected pattern is feasible, and this leads, as a direct consequence, to the improvement of the performance of the technique in terms of sensitivity also in correspondence to inhomogeneous surfaces. Finally, a preliminary test on a cylindrical surface with regions of different reflectivity was performed and initial capability of the proposed algorithm was assessed.

Next steps in the work will be to test the algorithm with very inhomogeneous surfaces from a reflectivity point of view as, for example, those connected with marbles.

Acknowledgements – This research was co-funded by Fondo di Sviluppo e Coesione 2007–2013 – APQ Ricerca Regione Puglia "Programma regionale a sostegno della specializzazione intelligente e della sostenibilità sociale ed ambientale" – FutureInResearch. Authors thank P. Pappalardi for his collaboration.

References

[1] SITNIK R., *A fully automatic 3D shape measurement system with data export for engineering and multimedia systems*, A dissertation submitted in partial fulfilment of the requirements for the degree of doctor of philosophy in the Warsaw University of Technology, Warsaw, 2002.

[2] BROGGIATO G.B., CAMPANA F., GERBINO S., MARTORELLI M., *Confronto tra diverse tecniche di digitalizzazione delle forme per il reverse engineering*, Giornale ATA **55**(7/8), 2002, pp. 256–266.

[3] HUYNH D.Q., OWENS R.A., HARTMANN P.E., *Calibrating a structured light stripe system: a novel approach*, International Journal of Computer Vision **33**(1), 1999, pp. 73–86, DOI: 10.1023/A:1008117315311.

[4] BARILE C., CASAVOLA C., PAPPALETTERA G., PAPPALETTERE C., *Residual stress measurement by electronic speckle pattern interferometry: a study of the influence of geometrical parameters*, Structural Integrity and Life **11**(3), 2011, pp. 177–182.

[5] BARILE C., CASAVOLA C., PAPPALETTERA G., PAPPALETTERE C., *Residual stress measurement by electronic speckle pattern interferometry: a study of the influence of analysis parameters*, Structural Integrity and Life **12**(3), 2012, pp. 159–163.

[6] MIAO H., QUAN C., TAY C.J., FU Y., WU X.P., *Optical edge projection for surface contouring*, Optics Communications **256**(1–3), 2005, pp. 16–23, DOI: 10.1016/j.optcom.2005.06.029.

[7] SALVI J., PAGÈS J., BATLLE J., *Pattern codification strategies in structured light systems*, Pattern Recognition **37**(4), 2004, pp. 827–849, DOI: 10.1016/j.patcog.2003.10.002.

[8] TALEBI R., ABDEL-DAYEM A., JOHNSON J., *3-D reconstruction of objects using digital fringe projection: survey and experimental study*, World Academy of Science, Engineering and Technology, International Journal of Mathematical and Computational Sciences **7**(6), 2013, pp. 1010–1019.

[9] SONG ZHANG, VAN DER WEIDE D., OLIVER J., *Superfast phase-shifting method for 3-D shape measurement*, Optics Express **18**(9), 2010, pp. 9684–9689, DOI: 10.1364/OE.18.009684.

[10] MING-JUNE TSAI, CHUAN-CHENG HUNG, *Development of a high-precision surface metrology system using structured light projection*, Measurement **38**(3), 2005, pp. 236–247, DOI: 10.1016/j.measurement.2005.07.014.

[11] Blahusch G., Eckstein W., Steger C., *Calibration of curvature of field for depth from focus*, ISPRS Archives **34**, 2003, pp. 173–177.

[12] Mora P., Mora L., *Le superfici architettoniche, materiale e colore*, Bollettino d'Arte Ministero per i Beni Culturali e le Attività Culturali, 35–36, 1984, pp. 115–118.

[13] Waddington C., Kofman J., *Analysis of measurement sensitivity to illuminance and fringe-pattern gray levels for fringe-pattern projection adaptive to ambient lighting*, Optics and Lasers in Engineering **48**(2), 2010, pp. 251–256, DOI: 10.1016/j.optlaseng.2009.07.001.

[14] Waddington C., Kofman J., *Modified sinusoidal fringe-pattern projection for variable illuminance in phase-shifting three-dimensional surface-shape metrology*, Optical Engineering **53**(8), 2014, article ID 084109, DOI: 10.1117/1.OE.53.8.084109.

[15] Hui Lin, Jian Gao, Guanjin Zhang, Xin Chen, Yunbo He, Yan Liu, *Review and comparison of high -dynamic range three-dimensional shape measurement techniques*, Journal of Sensors, Vol. 2017, 2017, article ID 9576850, DOI: 10.1155/2017/9576850.

[16] Das A., Kar A., Bhattacharyya D., *Elimination of specular reflection and identification of ROI: the first step in automated detection of cervical cancer using digital colposcopy*, 2011 IEEE International Conference on Imaging Systems and Techniques, 2011, pp. 237–241, DOI: 10.1109/IST.2011.5962218.

[17] Farid H., Adelson E.H., *Separating reflections and lighting using independent components analysis*, [In] *Proceedings. 1999 IEEE Computer Society Conference on Computer Vision and Pattern Recognition*, Vol. 1, 1999, pp. 262–267, DOI: 10.1109/CVPR.1999.786949.

[18] Liang-Chia Chen, Duc-Hieu Duong, Chin-Sheng Chen, *3-D surface profilometry for objects having extremely different reflectivity regions*, The 14th IFToMM World Congress, Taipei, Taiwan, October 25–30, 2015, DOI: 10.6567/IFToMM.14TH.WC.OS12.012.

[19] Waddington C., Kofman J., *Camera-independent saturation avoidance in measuring high-reflectivity-variation surfaces using pixel-wise composed images from projected patterns of different maximum gray level*, Optics Communications **333**, 2014, pp. 32–37, DOI: 10.1016/j.optcom.2014.07.039.

[20] Babaie G., Abolbashari M., Farahi F., *Dynamics range enhancement in digital fringe projection technique*, Precision Engineering, **39**, 2015, pp. 243–251, DOI: 10.1016/j.precisioneng.2014.06.007.

[21] Hui Lin, Jian Gao, Qing Mei, Yunbo He, Junxiu Liu, Xingjin Wang, *Adaptive digital fringe projection technique for high dynamic range three-dimensional shape measurement*, Optics Express **24**(7), 2016, pp. 7703–7718, DOI: 10.1364/OE.24.007703.

[22] Chi Zhang, Jing Xu, Ning Xi, Jianguo Zhao, Quan Shi, *A robust surface coding method for optically challenging objects using structured light*, IEEE Transactions on Automation Science and Engineering **11**(3), 2014, pp. 775–778, DOI: 10.1109/TASE.2013.2293576.

[23] Srinivasan V., Liu H.C., Halioua M., *Automated phase-measuring profilometry: a phase mapping approach*, Applied Optics **24**(2), 1985, pp. 185–188, DOI: 10.1364/AO.24.000185.

[24] Sitnik R., Kujawińska M., Woźnicki J.M., *Digital fringe projection system for large-volume 360-deg shape measurement*, Optical Engineering **41**(2), 2002, pp. 443–449, DOI: 10.1117/1.1430422.

Received December 21, 2017
in revised form April 6, 2018